

Wet deposition of fossil and non-fossil derived particulate carbon:

Insights from radiocarbon measurement

Yanlin Zhang^{1,2,5}, Mário Cerqueira³, Gary Salazar¹, Peter Zotter², Christoph Hueglin⁴,
Claudia Zellweger⁴, Casimiro Pio³, André S.H. Prévôt², Sönke Szidat¹

¹ Department of Chemistry and Biochemistry & Oeschger Centre for Climate Change Research, University of Bern, Freiestrasse 3, 3012 Bern, Switzerland

² Paul Scherrer Institute, 5232 Villigen-PSI, Switzerland

³ Department of Environment & Center for Environmental and Marine Studies (CESAM), University of Aveiro, 3810-193 Aveiro, Portugal

⁴ Laboratory for Air Pollution/Environmental Technology, Empa (Swiss Federal Laboratories for Materials Science and Technology), 8600 Dübendorf, Switzerland

⁵ now at Yale-NUIST Center on Atmospheric Environment, Nanjing University of Information Science and Technology, 210044 Nanjing, China

Accepted version

Published in

Atmospheric Environment 115 (2015), 257-262

<http://dx.doi.org/10.1016/j.atmosenv.2015.06.005>

This document is the accepted manuscript version of the following article:
Zhang, Y. L., Cerqueira, M., Salazar, G., Zotter, P., Hueglin, C., Zellweger, C., ... Szidat, S. (2015). wet deposition of fossil and non-fossil derived particulate carbon: insights from radiocarbon measurement. *Atmospheric Environment*, 115, 257-262. <https://doi.org/10.1016/j.atmosenv.2015.06.005>

This manuscript version is made available under the CC-BY-NC-ND 4.0 license
<http://creativecommons.org/licenses/by-nc-nd/4.0/>

1 **Abstract**

2 Radiocarbon (^{14}C) measurements of both organic carbon (OC) and elemental carbon (EC)
3 allow a more detailed source apportionment, leading to a full and unambiguous distinction
4 and quantification of the contributions from non-fossil and fossil sources. A thermal-
5 optical method with a commercial OC/EC analyzer to isolate water-insoluble OC (WIOC)
6 and EC for their subsequent ^{14}C measurement was applied for the first time to filtered
7 precipitation samples collected at a coastal site in Portugal and at a continental site in
8 Switzerland. Our results show that WIOC in precipitation is dominated by non-fossil
9 sources such as biogenic and biomass-burning emissions regardless of rain origins and
10 seasons, whereas EC sources are shared by fossil-fuel combustion and biomass burning.
11 In addition, monthly variation of WIOC in Switzerland was characterized by higher
12 abundance in warm than in cold seasons, highlighting the importance of biogenic
13 emissions to particulate carbon in rainwater. Samples with high particulate carbon
14 concentrations in Portugal were found to be associated with increased biogenic input.
15 Despite the importance of non-fossil sources, fossil emissions account for approximately
16 20% of particulate carbon in wet deposition for our study, which is in line with fossil
17 contribution in bulk rainwater dissolved organic carbon as well as aerosol WIOC and EC
18 estimated by the ^{14}C approach from other studies.

19

20 Keywords: Radiocarbon, Particulate carbon, Precipitation, Fossil, Non-fossil

21

22

23 **1. Introduction**

24 Carbonaceous particles (total carbon, TC) are of great importance due to effects
25 on human health and earth's climate (Pöschl, 2005; IPCC, 2013). Particulate carbon in
26 precipitation has been investigated in various locations across the globe, including sites
27 in urban, rural, mountain, coastal and marine areas. Wet deposition is known to be a key
28 scavenging (removing) process of carbonaceous particles (Fig. 1). Much of this research
29 has been focused on the abundance of different carbon fractions (elemental carbon, EC,
30 and water-insoluble organic carbon, WIOC), their spatial distribution, incorporation of
31 particles in hydrometeors and wet deposition fluxes (Cadle et al., 1980; Ducret and
32 Cachier, 1992; Chylek et al., 1999; Cerqueira et al., 2010). In contrast, rather less attention
33 has been paid to the identification of sources (e.g. fossil and non-fossil emissions) and the
34 assessment of their relative contribution to particulate carbon.

35 Radiocarbon (^{14}C) measurements have been widely used to distinguish
36 contemporary and fossil carbon in ambient air aerosol samples in either bulk TC (Szidat
37 et al., 2013; Zotter et al., 2014b) or in different carbonaceous fractions (Szidat et al., 2009;
38 Zhang et al., 2014a, 2014b). Source attribution is based on a simple model which assumes
39 that emissions from biogenic processes or biomass combustion are labelled with the
40 ambient $^{14}\text{C}/^{12}\text{C}$ ratio and emissions from fossil-fuel combustion contain no ^{14}C because
41 of the large age of this material (Currie, 2000).

42 To the best of our knowledge this approach has never been used in source
43 apportionment studies of WIOC and EC in precipitation samples (rain and snow),
44 although it was applied in some cases to deposited snow of ice core research (Jenk et al.,
45 2006; Cao et al., 2013) as well as total organic carbon (TOC) and dissolved organic
46 carbon (DOC) in rain (Raymond, 2005; Avery et al., 2006, 2013). One of the most
47 challenging problems of the method lies in lower concentration of particulate organic

48 carbon (POC) compared to DOC and offline separation methods for ^{14}C measurements in
49 water-insoluble total carbon (WITC) and, especially, different carbon fractions such as
50 EC and WIOC. Thermal-optical analysis (TOA) is one of the most commonly used
51 methods for measuring the OC/EC concentration in aerosol and precipitation samples. In
52 most TOA methods such as NIOSH, IMPROVE and EUSAAR protocols, the filter
53 sample is heated sequentially in an inert (He) and oxidative (He/O₂ mixture) atmosphere
54 (Cavalli et al., 2010). Ideally, OC and EC are released in each step separately. However,
55 part of OC is formed as charring (EC-like material that is refractory and light-absorbing),
56 which occurs in the first step and is mistakenly detected as EC in the second step.
57 Therefore, a laser is used to monitor the filter transmittance throughout analysis to
58 account for the charring contribution. The charring correction is then carried out to
59 quantify OC/EC mass concentration by assigning a split point at the time when the
60 transmittance returns to its initial value during the He/O₂ step (Cavalli et al., 2010).
61 However, the charring correction is not feasible for ^{14}C analysis of OC and EC, since this
62 requires a physical separation of the two fractions and the split point is unknown before
63 measurement. This was recently improved by a thermaloptical method utilizing both the
64 special thermal and optical properties of OC and EC, thereby optimizing both the
65 quantification and isolation of OC and EC (Zhang et al., 2012).

66 Aerosol pollution from wood burning has recently been recognized in large-scale
67 areas of Europe including Scandinavia, Portugal and alpine regions, as well as in major
68 European cities such as London, Paris and Berlin despite the importance of fossil-fuel
69 emissions (Szidat et al., 2009; Borrego et al., 2010; Fuller et al., 2013, 2014; Herich et
70 al., 2014; Zotter et al., 2014a). However, current understanding on the impact of fossil
71 versus biomass burning to aerosols is incomplete, since the source of WITC in wet
72 deposition, a major removal process of particulate carbon in the atmosphere (Ducret and

73 Cachier, 1992), are still not well constrained. Therefore, the motivation for the present
74 study was (1) to adapt a method that has been successfully applied for ^{14}C analysis of
75 atmospheric aerosols to the quantification of ^{14}C in particulate carbon extracted from
76 rainwater and (2) to quantify fossil and non-fossil contributions to particulate carbon
77 including OC and EC in precipitation from samples collected in Portugal and Switzerland.
78 This study also provides new insights into the wet deposition of particulate carbon emitted
79 by both fossil and non-fossil sources, and improves our understanding of the role of
80 atmospheric particulate carbon in the models of the global carbon cycle.

81 **2. Experimental**

82 *2.1 Measurement sites and analytical method*

83 Investigations were carried out at two different sites, Aveiro in Portugal ($40^{\circ} 38' 07''\text{N}$
84 and $8^{\circ} 39' 35''\text{W}$) and Dübendorf ($47^{\circ} 24' 11''\text{N}$ and $8^{\circ} 36' 48''\text{W}$) in Switzerland.
85 Sampling at Aveiro was conducted at the University of Aveiro campus, located at the
86 southwestern rim of the city of Aveiro, western coast of Portugal. The campus is about 7
87 km from the sea-side and there are no significant pollution sources in the area between it
88 and the ocean. The roof of a small container placed near the campus meteorological
89 station was used as a platform to collect rain samples, at about 4 m above ground level.
90 Sampling at Dübendorf was performed on the premises of EMPA located outside of
91 Dübendorf, a city with 25,000 inhabitants and a suburb of the city of Zurich (400,000
92 inhabitants). The site therefore is of suburban type located 432 m a.s.l. in the northern
93 part of Switzerland. The rain samples have been collected at 2 m above ground level.

94 *2.2 Sampling method*

95 Rainwater samples in Portugal were collected on an event basis from mid-February until
96 the end of April 2011 with an Eigenbrodt model UNS130/E automatic wet-only collector.
97 The sampler consisted of a glass funnel with an open area of 500 cm^2 , connected to a 5 L

98 glass storage bottle, a movable lid and a precipitation sensor to control start and stop of
99 each collection period. Prior to use, all the collector components that could come in
100 contact with samples were cleaned with soap and water, followed by rinsing of them with
101 distilled and deionized water. Rainwater samples at Dübendorf, Switzerland were
102 collected on a daily basis from April 2012 to March 2013 with a Digital model DRA-92
103 HK wet-only collector. The sampler consists of a Teflon-coated funnel with an open area
104 of 500 cm². The rain samples were collected in storage bottles (polyethylene, 250 mL)
105 which were automatically changed at midnight or when they were full. The funnel and
106 the subsequent Teflon tube have monthly been cleaned with ultrapure water, the storage
107 bottles have been rinsed with ultrapure water before they were used. One field blank at
108 each site was prepared by pouring ultrapure water (50 mL) through the sampling device,
109 collecting the rinsate in a storage bottle and, after staying one day inside the closed
110 collector, processed under the same conditions as samples.

111 *2.3 Filtration*

112 The particulate carbon in the rainwater samples were collected on prebaked quartz fibre
113 filter (Pallflex Tissuquartz, 2500QAO-UP) with a diameter of 10-11 mm by filtration
114 using vacuum suction. Prior to the use of containers and the filtration funnel, they were
115 rinsed three times with ~25 mL ultra-pure water with low carbon impurity in order to
116 reduce the blank. A series of three filters were used to collect particles to increase
117 filtration efficiency. The filtration efficiency with a similar approach was reported to be
118 $92 \pm 7\%$ using prepared standards of known quantities of soot in water (Hadley et al.,
119 2008). Filtered water volumes were typically in the range of 250-700 mL. For samples
120 from Portugal (n = 7), daily rain samples were filtered at the University of Aveiro before
121 sending to the University of Bern for ¹⁴C analysis by express mail in a cooled container.

122 For samples from Switzerland (n = 12), rain events were pooled per month for filtration,
123 which was conducted at the University of Bern.

124 *2.4 Determination and separation of different carbonaceous particle fractions*

125 OC and EC fractions extracted from precipitation samples were isolated by the Swiss_4S
126 protocol for subsequent ^{14}C measurement. This method was first described in Zhang et
127 al. (2012) for analyzing ambient aerosols samples and recently applied for particulate
128 carbon extracted from firn/ice samples by Cao et al. (2013). In brief, WIOC is combusted
129 in pure oxygen at 375 °C for 180 s in step one and subsequently EC is combusted in pure
130 oxygen at 760 °C for 120 s in step four after complete OC removal in pure oxygen at 475
131 °C for 120 s (step two) and in helium at 650 °C for 180 s (step three). The evolving CO_2
132 is quantified by a non-dispersive infrared (NDIR) detector, separated from interfering
133 reaction gases, cryotrapped and sealed in glass ampoules for ^{14}C measurements. By using
134 the Sunset OC/EC analyzer, which monitors the filter optical properties during the
135 combustion with a laser, the quantification of the EC losses before step four is also
136 possible. Therefore, mass concentration of WIOC, EC and WITC can be quantified as
137 well. A good agreement of carbon mass determination by the Swiss_4S and the
138 EUSAAR_2 protocol was previously reported for aerosol samples (Zhang et al., 2012).
139 The extent of charring formation during the thermal treatment can be reduced by using
140 pure oxygen instead of helium, which is evident by the comparison of thermograms
141 applying different protocols (see Supplemental material, Figure S1). However, substantial
142 OC charring still occurs, sometimes larger than 10% of EC mass, which results in a
143 positive bias of the ^{14}C measurement of the EC fraction, as OC and EC often differ in
144 their ^{14}C content (Szidat et al., 2009; Zhang et al., 2013). Since some charred material is
145 very likely removed during step three before the EC step, we assume that $50 \pm 15\%$ of

146 the charred OC remains in the EC fraction. Therefore, the fraction of modern (f_M , see Sec
147 2.4) of EC ($f_{M,EC}$) as corrected for charring ($f_{M,EC,final}$) is as follows:

$$148 \quad f_{M, EC \text{ corr}} = (mC_{EC} * f_{M, EC} - mC_{charring} * f_{M, charring}) / (mC_{EC} - mC_{charring}),$$

149 where $f_{M,EC}$ and $f_{M,charring}$ denote the f_M measured and mC_{EC} and $mC_{charring}$ the carbon
150 mass for EC and charred OC, respectively.

151 $f_{M,charr}$ is assumed to equate to the measured $f_{M,OC}$, as charred OC is part of the OC
152 fraction. The typical uncertainties of source apportionment results arise from analytical
153 uncertainties (i.e. OC/EC mass and ^{14}C measurements), blank/charring correction and
154 the variability of reference $f_{M,nf}$ values (see Sec 2.5) approximately amounted to $\pm 20\%$,
155 $\pm 20\%$, $\pm 15\%$ and $\pm 10\%$ for fossil EC, non-fossil EC, fossil OC and non-fossil OC,
156 respectively.

157 2.5 ^{14}C analysis

158 ^{14}C analyses of CO_2 produced samples from OC/EC analyzer were measured with the
159 Mini Carbon Dating System (MICADAS) at the Laboratory for the Analysis of
160 Radiocarbon with AMS and at ETH Zurich, both of which using a gas ion source, which
161 allows direct CO_2 injection after dilution with He (Wacker et al., 2013; Szidat et al., 2014).
162 ^{14}C results are usually expressed as fractions of modern (f_M), which were further
163 converted to fraction of non-fossil (f_{NF}) by dividing by f_M reference values for
164 contemporary carbon for the source apportionment of non-fossil and fossil carbon. f_M
165 reference value of OC ($f_{M,ref}$) were estimated as 1.08 ± 0.05 for non-fossil continental
166 sources for both sites according to (Zhang et al., 2014a). For samples influenced by
167 marine sources at the Portugal sampling site, this reference value was estimated as 0.98
168 ± 0.04 (see Sec 3.1.1. and Figure S2) following the concept of (Ceburnis et al., 2011),
169 which is currently the best available approach for this determination. It should be noted
170 that the uncertainty of source-specific contributions are dependent on the selected f_M

171 reference values. By varying reference f_M by ± 0.05 , the uncertainty is typically within
172 5%. A mass-dependent blank correction is applied to the measured f_M values for OC
173 according to an isotopic mass balance approach. The f_M and OC value of the blank was
174 0.59 ± 0.02 and $1.2 \pm 0.8 \mu\text{gC}$ per filtration, respectively. No blank correction was carried
175 out for ^{14}C measurement of EC as carbon amount of blank EC ($0.4 \pm 0.4 \mu\text{gC}$) was below
176 the detection limit ($\sim 2\text{-}3 \mu\text{gC}$) of the ^{14}C analysis.

177 **3. Results and discussion**

178 *3.1 Particulate OC and EC levels in precipitation*

179 *3.1.1 Aveiro, Portugal*

180 Seven rain samples were characterized for their WITC concentrations and the
181 corresponding ^{14}C values. Details about rain events are reported in Table S1 and
182 analytical results are presented in Fig. 2. Backward air mass trajectories arriving at Aveiro
183 during the rain events generated with the HYSPLIT model are shown in Figure S2.
184 According to air mass origins, 7 samples were classified into 2 types: marine (TYPE1:
185 samples AVE1 to AVE5) where the airmass travelling over the ocean and continental
186 influenced rainwater (TYPE2: samples AVE6 and AVE7) with a mixture of continental
187 and marine influences. The average WITC was $128.4 \pm 87.7 \mu\text{g/L}$ and $272.1 \pm 42.3 \mu\text{g/L}$
188 for marine and continental influenced rainwater, respectively. The lowest WITC
189 concentrations were found in rain samples AVE1, AVE3 and AVE5, with a mean of 66
190 $\pm 12 \mu\text{g/L}$. With a similar air mass origin (Figure S2), WITC in sample AVE2 and AVE4
191 was significantly increased. These two samples were likely influenced by additional local
192 emissions. Indeed, plant debris (or detritus) was visible after filtration of the sample
193 AVE2, explaining the high WITC concentration. This sample was taken under conditions
194 with elevated wind speed compared to the other samples (Table S1), which might have
195 been the cause of a significant input of plant debris into local air. On the other hand,

196 pollen grains were observed after filtration of sample AVE4. Marine pine (*Pinus pinaster*)
197 is the dominant tree in north-western Portugal and airborne pollen from this species is
198 known to have a seasonal variation with a peak during March (Sousa et al., 2008). Pollen
199 grains of marine pine deposit intensely at this time of the year and are frequently observed
200 as a yellow dust accumulated on outside surfaces. In addition, the average WIOC/EC ratio
201 (5.7) of samples AVE2 and AVE4 were significantly higher than that (3.2) in samples
202 AVE1, AVE3 and AVE5, indicating that the larger TC abundance for samples AVE2 and
203 AVE4 is rather due to biogenic/biomass sources than anthropogenic sources. The higher
204 WITC concentrations detected in TYPE2 were probably due to higher aerosol pollution
205 in continental air-mass origins. Actually, during the rain event of 18-19 of April (sample
206 AVE6), air masses originated from the western coast of Africa and were transported over
207 densely populated areas in coastal Portugal before arriving at the sampling site. Sample
208 AVE7 reflects the influence of two types of transport: whereas air masses arrived from
209 northwest, after crossing France and Spain, during the first half of the sampling period,
210 the second half was dominated by air-mass transport over northern Africa, southern Spain
211 and inland Portugal. However, the source of the continental-influenced samples remains
212 unknown, which we will discuss below (Sec 3.2.1).

213 *3.1.2 Dübendorf, Switzerland*

214 WITC concentration levels in the precipitation samples from Dübendorf ranged from 73
215 $\mu\text{g/L}$ to 228 $\mu\text{g/L}$, with an annual average of $147 \pm 58 \mu\text{g/L}$ (Figure 3). The monthly WIOC
216 concentrations were lower in cold seasons than in warm seasons, associated with larger
217 biogenic emissions in both spring and summer. Although wood burning in winter is a
218 dominant contributor of airborne OC in Switzerland (Zotter et al., 2014a), this may not
219 affect particulate OC fraction in precipitation significantly, as a large fraction of
220 woodburning OC may be dissolved into the rainwater due to high water solubility and

221 thus mainly exist in the rainwater DOC fraction. Previous studies reported higher levels
222 of DOC in rainwater in warm seasons in other regions, such as coastal New Zealand and
223 North Carolina, USA, as biogenic emissions from vegetation is largely controlled by
224 seasonality (Willey et al., 2000; Kieber et al., 2002). However, this seasonality was not
225 found for EC, as this fraction is only produced by fossil-fuel combustion and biomass
226 burning, but not by biogenic emissions. Actually, monthly EC concentrations showed
227 relatively small variations throughout the year in contrast with the fact that EC abundance
228 in ambient aerosol samples has been reported to be highest in winter due to accumulation
229 during winter-smog episodes and enhanced residential wood burning in Switzerland
230 (Herich et al., 2011). It should be noted that precipitation seldom occurs during winter-
231 smog episodes and most precipitation events in winter are snow events so that different
232 wet scavenging efficiencies between rain and snow events may play a role on wet
233 deposition of EC. Correlation with the amount of precipitation was neither observed for
234 WITC, WIOC, or EC concentrations, and also not for their ^{14}C level, probably because of
235 pooling monthly averaged samples.

236 *3.2 Sources of particulate carbon in precipitation: fossil vs. non-fossil sources*

237 *3.2.1 Aveiro, Portugal*

238 In general, both natural and anthropogenic sources including biogenic emissions, biomass
239 burning and fossil-fuel combustion can contribute to rainwater particulate carbon. In this
240 work, the source apportionment of particulate carbon in precipitation was made based on
241 ^{14}C measurements, assuming non-fossil carbon has the same f_M as the contemporary
242 atmosphere and fossil fuel carbon is devoid of ^{14}C . As samples AVE2 and AVE4 were
243 influenced by large primary biogenic particulate matter, ^{14}C measurement has only been
244 performed on bulk WITC, because large primary biogenic particulate matter may
245 significantly affect the WIOC/EC separation. The average non-fossil contribution to

246 WIOC is 84% and 91% for marine and continental influenced rainwater, respectively.
247 The fossil components found in rainwater at this coastal site likely reflect the export of
248 fossil emissions from the North American continent, the input of emissions from ship and
249 aircraft emissions as well as local traffic emissions. ^{14}C measurement of samples with the
250 highest WITC content (samples AVE2 and AVE4) confirm, however, that these two
251 samples are indeed influenced by nonfossil emissions (i.e. primary biogenic emissions).
252 Non-fossil contributions (i.e. biomass burning) to EC were on average $52\% \pm 2\%$ and 58%
253 $\pm 2\%$ for TYPE1 and TYPE2, respectively, which was lower than the corresponding non-
254 fossil fraction in OC with average contributions of $84\% \pm 2\%$ and $90\% \pm 2\%$. Biomass
255 burning EC mainly originates from residential wood burning for heating and/or open
256 biomass burning. Wood burning has been reported to be a considerable contributor to EC
257 by many previous studies conducted in Europe (Szidat et al., 2009; Fuller et al., 2014;
258 Zotter et al., 2014a). The MODIS fire counts map
259 (<https://firms.modaps.eosdis.nasa.gov/firemap/>, Figure S3) during April shows that
260 intensive open biomass-burning activities took place in upwind direction of and/or in
261 surrounding regions of the sampling site, which could be another explanation of the
262 enrichment of non-fossil carbon in both OC and EC fractions of samples AVE6 and
263 AVE7. Therefore, high abundance particulate OC found in continental influenced
264 rainwater is not due to larger urban fossil emissions, but due to enhanced biogenic and
265 biomass-burning emissions according to ^{14}C results in both WIOC and EC fractions.

266 *3.2.2 Dübendorf, Switzerland*

267 On average, non-fossil sources contributed $84 \pm 5\%$ to OC on an annual average, which
268 was always higher than non-fossil EC with a mean contribution of $48 \pm 7\%$ (Fig. 3). This
269 finding agrees with the fact that OC/EC emissions ratios are higher in biogenic or biomass
270 burning sources than those in fossil fuel emissions (i.e. mainly vehicular emissions in

271 Europe) (Pio et al., 2011). A notable seasonality was not found for relative fossil and non-
272 fossil contributions to OC, whereas non-fossil EC fraction was slightly higher in winter
273 than other seasons due to larger wood burning emission for heating during cold period
274 (Zhang et al., 2013; Zotter et al., 2014a). The high non-fossil fractions in rainwater WIOC
275 are attributed to biogenic and wood burning emissions. Based on a carbon isotope mass
276 balance (i.e. $f_{NF}(WITC) \cdot mC_{WITC} = f_{NF}(OC) \cdot mC_{OC} + f_{NF}(EC) \cdot mC_{EC}$), the annual-average
277 non-fossil contribution to WITC was $79 \pm 5\%$ with a consistent non-fossil predominance
278 throughout the year, which dominated the wet deposition of atmospheric organic aerosols.
279 Previous studies also found similar ^{14}C values for bulk rain DOC, although there are no
280 studies reporting ^{14}C measurements on POC in rainwater to the best of our knowledge.
281 For example, ^{14}C measurements of rain DOC from two sites in the northeast USA suggest
282 approximately 78% and 85% was non-fossil origin, respectively (Raymond, 2005; Avery
283 et al., 2006).

284 *3.3 Summary and discussions*

285 This paper reports the first successful application of radiocarbon (^{14}C) analysis to water-
286 insoluble particles extracted from precipitation. Based on ^{14}C measurement of particulate
287 OC and EC of rainwater samples at a coastal site in Portugal and a continental site in
288 Switzerland, particulate carbon in precipitation is dominated by non-fossil sources, such
289 as biogenic and biomass-burning emissions regardless of season as well as air-mass and
290 rain origins. It should be worth noting that non-fossil contributions in total particulate
291 carbon in precipitation in both studied sites were higher than those reported in airborne
292 aerosol samples. For example, Gelencsér et al. (2007) showed that non-fossil contribution
293 fraction was on average 73% and 81% of TC in $PM_{2.5}$ aerosol samples collected during
294 summer and winter at Aveiro, Portugal, respectively, (Gelencsér et al., 2007), slightly
295 lower than our finding (averaged to 81%) in rainwater samples. Recently, a yearly cycle

296 of ^{14}C measurement of OC and EC of PM_{10} aerosol samples was investigated at an urban
297 background station in Zurich, Switzerland (Zotter et al., in preparation). Non-fossil
298 contributions to TC is on average 15% lower compared to those extracted from rainwater
299 samples collected at Dübendorf, 6 km north of Zurich. In addition, they found a very clear
300 seasonal cycle for relative non-fossil contribution of EC (ranging from 9 to 50%) in PM_{10}
301 aerosol samples, whereas in the precipitation analysed in this study, less seasonal
302 variation (ranging from 37 to 59%) was observed. We hypothesize that particles emitted
303 from biomass-burning processes may be coated with more hydrophilic compounds such
304 as inorganic substances and oxidized organic aerosols, which may increase the wet
305 removal efficiency of non-fossil particles. By examining aerosol size distributions and
306 BC coating properties sampled in three Canadian boreal biomass burning plumes, Taylor
307 et al. (2014) have also demonstrated that less coated EC particles are less effectively
308 removed by wet deposition (Taylor et al., 2014). Moreover, it should be emphasized that
309 precipitation includes larger particulate matter than PM_{10} aerosol, which may have an
310 influence on the outcome of the ^{14}C source apportionment, as we recently showed for fine
311 and coarse aerosol fractions (Zhang et al., 2013). Further experiments with simultaneous
312 measurements on both aerosol and precipitation samples are required to study wet
313 scavenging processes and mechanisms for carbonaceous particles from both fossil and
314 non-fossil origins.

315 The findings from our study suggest that wet deposition preferentially removes non-fossil
316 derived carbonaceous particles. Despite of the importance of non-fossil sources, fossil
317 emissions account for approximately 20% of total particulate carbon in wet deposition for
318 our study, which is in line with fossil contribution in bulk rainwater DOC as well as
319 aerosol WIOC and EC estimated by the ^{14}C approach from other studies (Raymond, 2005;
320 Avery et al., 2006; Szidat et al., 2009; Zotter et al., 2014a). Based on literature studies

321 and our observations, a very gross estimation of wet-deposited fossil-derived carbon was
322 also carried out. By assuming 430 Tg C/y is removed from the atmosphere by rainwater
323 DOC (Willey et al., 2000) and multiplying it by the average POC percentages (15%) in
324 TOC (the sum of POC and DOC) from previous studies (Sempere and Kawamura, 1996;
325 Willey et al., 2000) as well as an average fossil contribution (20%) to POC from our
326 current study could approximately yield a net removal of 12.9 Gt fossil-derived C per
327 year in the particulate phase via wet deposition. This gross estimation is within the upper
328 range of bottom-up primary organic aerosols from fossil fuel emissions of 5-15 TgC/y
329 (Bond et al., 2004; Hallquist et al., 2009), suggesting that the majority of fossil-derived
330 primary organic aerosols are removed by wet deposition. Therefore, fossil-derived
331 particulate carbon can be transferred between different ecosystem (e.g. from land to ocean
332 or from ocean to land) via wet deposition, and it can play an important role on the Earth's
333 environment and human health via biogeochemical carbon cycle.

334 **Acknowledgements**

335 This study was financially supported by the European Regional Fund Development
336 through the program COMPETE - *Programa Operacional Factores de Competividade*
337 and by the Portuguese Foundation for Science and Technology through the project “Wet
338 deposition of particulate carbon over the Northeast Atlantic region”
339 (PTDC/AMB/66198/2006). The authors gratefully acknowledge the NOAA Air
340 Resources Laboratory (ARL) for the provision of the HYSPLIT transport and dispersion
341 model used in this publication. Also acknowledged is L. Wacker (ETH Zurich) for
342 making available the MICADAS for some of the ^{14}C measurements in this study. Yan-
343 Lin Zhang also acknowledges the “Mobility Fellowship” from Swiss National Science
344 Foundation (152095) and the Startup Foundation for Introducing Talent of NUIST
345 (2015r023).

346 **References**

- 347 Avery, G.B., Willey, J.D., Kieber, R.J., 2006. Carbon isotopic characterization of
348 dissolved organic carbon in rainwater: terrestrial and marine influences. *Atmos.*
349 *Environ.* 40, 7539-7545.
- 350 Avery, G.B., Biswas, K.F., Mead, R., Southwell, M., Willey, J.D., Kieber, R.J.,
351 Mullaugh, K.M., 2013. Carbon isotopic characterization of hydrophobic dissolved
352 organic carbon in rainwater. *Atmos. Environ.* 68, 230-234.
- 353 Bond, T.C., Streets, D.G., Yarber, K.F., Nelson, S.M., Woo, J.H., Klimont, Z., 2004. A
354 technology-based global inventory of black and organic carbon emissions from
355 combustion. *J. Geophys. Res.* 109, D14203.
- 356 Borrego, C., Valente, J., Carvalho, A., Sa, E., Lopes, M., Miranda, A.I., 2010.
357 Contribution of residential wood combustion to PM10 levels in Portugal. *Atmos.*
358 *Environ.* 44, 642-651.
- 359 Cadle, S.H., Groblicki, P.J., Stroup, D.P., 1980. Automated carbon analyzer for
360 particulate samples. *Anal. Chem.* 52, 2201-2206.
- 361 Cao, F., Zhang, Y.-L., Szidat, S., Zapf, A., Wacker, L., Schwikowski, M., 2013.
362 Microgram-level radiocarbon determination of carbonaceous particles in firn and ice
363 samples: pretreatment and OC/EC separation. *Radiocarbon* 55, 383-390.
- 364 Cavalli, F., Viana, M., Yttri, K.E., Genberg, J., Putaud, J.P., 2010. Toward a
365 standardised thermal-optical protocol for measuring atmospheric organic and elemental
366 carbon: the EUSAAR protocol. *Atmos. Meas. Tech.* 3, 79-89.
- 367 Ceburnis, D., Garbaras, A., Szidat, S., Rinaldi, M., Fahrni, S., Perron, N., Wacker, L.,
368 Leinert, S., Remeikis, V., Facchini, M.C., Prevot, A.S.H., Jennings, S.G., Ramonet, M.,
369 O'Dowd, C.D., 2011. Quantification of the carbonaceous matter origin in submicron
370 marine aerosol by ^{13}C and ^{14}C isotope analysis. *Atmos. Chem. Phys.* 11, 8593-8606.
- 371 Cerqueira, M., Pio, C., Legrand, M., Puxbaum, H., Kasper-Giebl, A., Afonso, J.,
372 Preunkert, S., Gelencser, A., Fialho, P., 2010. Particulate carbon in precipitation at
373 European background sites. *J. Aerosol Sci.* 41, 51-61.
- 374 Chylek, P., Kou, L., Johnson, B., Boudala, F., Lesins, G., 1999. Black carbon
375 concentrations in precipitation and near surface air in and near Halifax, Nova Scotia.
376 *Atmos. Environ.* 33, 2269-2277.
- 377 Currie, L.A., 2000. Evolution and multidisciplinary frontiers of ^{14}C aerosol science.
378 *Radiocarbon* 42, 115-126.
- 379 Ducret, J., Cachier, H., 1992. Particulate carbon content in rain at various temperate and
380 tropical locations. *J. Atmos. Chem.* 15, 55-67.
- 381 Fuller, G.W., Sciare, J., Lutz, M., Moukhtar, S., Wagener, S., 2013. New Directions:
382 time to tackle urban wood burning? *Atmos. Environ.* 68, 295-296.
- 383 Fuller, G.W., Tremper, A.H., Baker, T.D., Yttri, K.E., Butterfield, D., 2014.
384 Contribution of wood burning to PM10 in London. *Atmos. Environ.* 87, 87-94.
- 385 Gelencsér, A., May, B., Simpson, D., Sánchez-Ochoa, A., Kasper-Giebl, A., Puxbaum,
386 H., Caseiro, A., Pio, C., Legrand, M., 2007. Source apportionment of PM2.5 organic
387 aerosol over Europe: primary/secondary, natural/anthropogenic, and fossil/biogenic
388 origin. *J. Geophys. Res.* 112, D23S04.

389 Hadley, O.L., Corrigan, C.E., Kirchstetter, T.W., 2008. Modified thermal-optical
390 analysis using spectral absorption selectivity to distinguish black carbon from pyrolyzed
391 organic carbon. *Environ. Sci. Technol.* 42, 8459-8464.

392 Hallquist, M., Wenger, J.C., Baltensperger, U., Rudich, Y., Simpson, D., Claeys, M.,
393 Dommen, J., Donahue, N.M., George, C., Goldstein, A.H., Hamilton, J.F., Herrmann,
394 H., Hoffmann, T., Iinuma, Y., Jang, M., Jenkin, M.E., Jimenez, J.L., Kiendler-Scharr,
395 A., Maenhaut, W., McFiggans, G., Mentel, T.F., Monod, A., Prevot, A.S.H., Seinfeld,
396 J.H., Surratt, J.D., Szmigielski, R., Wildt, J., 2009. The formation, properties and impact
397 of secondary organic aerosol: current and emerging issues. *Atmos. Chem. Phys.* 9,
398 5155-5236.

399 Herich, H., Hueglin, C., Buchmann, B., 2011. A 2.5 year's source apportionment study
400 of black carbon from wood burning and fossil fuel combustion at urban and rural sites
401 in Switzerland. *Atmos. Meas. Tech.* 4, 1409-1420.

402 Herich, H., Gianini, M.F.D., Piot, C., Mocnik, G., Jaffrezo, J.L., Besombes, J.L., Prevot,
403 A.S.H., Hueglin, C., 2014. Overview of the impact of wood burning emissions on
404 carbonaceous aerosols and PM in large parts of the Alpine region. *Atmos. Environ.* 89,
405 64-75.

406 IPCC, 2013. In: Stocker, T.F., Qin, D., Plattner, G.-K., Tignor, M., Allen, S.K.,
407 Boschung, J., Nauels, A., Xia, Y., Bex, V., Midgley, P.M. (Eds.), *Climate Change 2013:*
408 *the Physical Science Basis. Contribution of Working Group I to the Fifth Assessment*
409 *Report of the Intergovernmental Panel on Climate Change.* Cambridge University Press,
410 Cambridge, United Kingdom and New York, NY, USA, p. 1533.

411 Jenk, T.M., Szidat, S., Schwikowski, M., Gaggeler, H.W., Brutsch, S., Wacker, L.,
412 Synal, H.A., Saurer, M., 2006. Radiocarbon analysis in an Alpine ice core: record of
413 anthropogenic and biogenic contributions to carbonaceous aerosols in the past (1650-
414 1940). *Atmos. Chem. Phys.* 6, 5381-5390.

415 Kieber, R.J., Peake, B., Willey, J.D., Avery, G.B., 2002. Dissolved organic carbon and
416 organic acids in coastal New Zealand rainwater. *Atmos. Environ.* 36, 3557-3563.

417 Pio, C., Cerqueira, M., Harrison, R.M., Nunes, T., Mirante, F., Alves, C., Oliveira, C.,
418 de la Campa, A.S., Artinano, B., Matos, M., 2011. OC/EC ratio observations in Europe:
419 re-thinking the approach for apportionment between primary and secondary organic
420 carbon. *Atmos. Environ.* 45, 6121-6132.

421 Pöschl, U., 2005. Atmospheric aerosols: composition, transformation, climate and
422 health effects. *Angew. Chem. Int. Ed.* 44, 7520-7540.

423 Raymond, P.A., 2005. The composition and transport of organic carbon in rainfall:
424 insights from the natural. *Geophys. Res. Lett.* 32, L14402.

425 Sempere, R., Kawamura, K., 1996. Low molecular weight dicarboxylic acids and
426 related polar compounds in the remote marine rain samples collected from western
427 Pacific. *Atmos. Environ.* 30, 1609-1619.

428 Sousa, S.I.V., Martins, F.G., Pereira, M.C., Alvim-Ferraz, M.C.M., Ribeiro, H.,
429 Oliveira, M., Abreu, I., 2008. Influence of atmospheric ozone, PM10 and
430 meteorological factors on the concentration of airborne pollen and fungal spores.
431 *Atmos. Environ.* 42, 7452-7464.

432 Szidat, S., Ruff, M., Perron, N., Wacker, L., Synal, H.-A., Hallquist, M., Shannigrahi,
433 A.S., Yttri, K.E., Dye, C., Simpson, D., 2009. Fossil and non-fossil sources of organic

434 carbon (OC) and elemental carbon (EC) in Goeteborg, Sweden. *Atmos. Chem. Phys.* 9,
435 1521-1535.

436 Szidat, S., Bench, G., Bernardoni, V., Calzolari, G., Czimczik, C.I., Derendorp, L.,
437 Dusek, U., Elder, K., Fedi, M., Genberg, J., Gustafsson, O., Kirillova, E., Kondo, M.,
438 McNichol, A.P., Perron, N., Santos, G.M., Stenstrom, K., Swietlicki, E., Uchida, M.,
439 Vecchi, R., Wacker, L., Zhang, Y.L., Prevot, A.S.H., 2013. Intercomparison of ¹⁴C
440 analysis of carbonaceous aerosols: exercise 2009. *Radiocarbon* 55, 1496-1509.

441 Szidat, S., Salazar, G.A., Vogel, E., Battaglia, M., Wacker, L., Synal, H.-A., Türler, A.,
442 2014. ¹⁴C analysis and sample preparation at the new Bern laboratory for the analysis of
443 radiocarbon with AMS (LARA). *Radiocarbon* 56, 561-566.

444 Taylor, J.W., Allan, J.D., Allen, G., Coe, H., Williams, P.I., Flynn, M.J., Breton, M.L.,
445 Muller, J.B.A., Percival, C.J., Oram, D., Forster, G., Lee, J.D., Rickard, A.R., Palmer,
446 P.I., 2014. Size-dependent wet removal of black carbon in Canadian biomass burning
447 plumes. *Atmos. Chem. Phys. Discuss.* 14, 19469-19513.

448 Wacker, L., Fahrni, S.M., Hajdas, I., Molnar, M., Synal, H.A., Szidat, S., Zhang, Y.L.,
449 2013. A versatile gas interface for routine radiocarbon analysis with a gas ion source.
450 *Nucl. Instrum. Meth. B* 294, 315-319.

451 Willey, J.D., Kieber, R.J., Eyman, M.S., Avery, G.B., 2000. Rainwater dissolved
452 organic carbon: concentrations and global flux. *Glob. Biogeochem. Cycles* 14, 139-148.

453 Zhang, Y.-L., Li, J., Zhang, G., Zotter, P., Huang, R.-J., Tang, J.-H., Wacker, L., Prévôt,
454 A.S.H., Szidat, S., 2014a. Radiocarbon-based source apportionment of carbonaceous
455 aerosols at a regional background site on hainan Island, South China. *Environ. Sci.*
456 *Technol.* 48, 2651-2659.

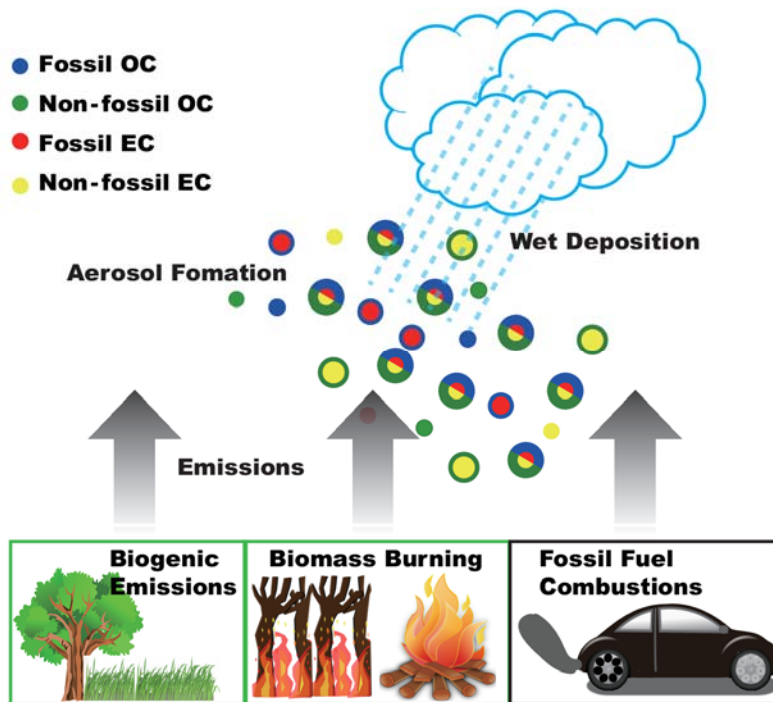
457 Zhang, Y.-L., Liu, J.-W., Salazar, G.A., Li, J., Zotter, P., Zhang, G., Shen, R.-R.,
458 Schäfer, K., Schnelle-Kreis, J., Prévôt, A.S.H., Szidat, S., 2014b. Micro-scale (μg)
459 radiocarbon analysis of water-soluble organic carbon in aerosol samples. *Atmos.*
460 *Environ.* 97, 1-5.

461 Zhang, Y.L., Perron, N., Ciobanu, V.G., Zotter, P., Minguillón, M.C., Wacker, L.,
462 Prévôt, A.S.H., Baltensperger, U., Szidat, S., 2012. On the isolation of OC and EC and
463 the optimal strategy of radiocarbon-based source apportionment of carbonaceous
464 aerosols. *Atmos. Chem. Phys.* 12, 10841-10856.

465 Zhang, Y.L., Zotter, P., Perron, N., Prévôt, A.S.H., Wacker, L., Szidat, S., 2013. Fossil
466 and non-fossil sources of different carbonaceous fractions in fine and coarse particles by
467 radiocarbon measurement. *Radiocarbon* 55, 1510-1520.

468 Zotter, P., Ciobanu, V.G., Zhang, Y.L., El-Haddad, I., Macchia, M., Daellenbach, K.R.,
469 Salazar, G.A., Huang, R.-J., Wacker, L., Hueglin, C., Piazzalunga, A., Fermo, P.,
470 Schwikowski, M., Baltensperger, U., Szidat, S., Prévôt, A.S.H., 2014a. Radiocarbon
471 analysis of elemental and organic carbon in Switzerland during winter-smog episodes
472 from 2008 to 2012 - Part 1: source apportionment and spatial variability. *Atmos. Chem.*
473 *Phys. Discuss.* 14, 15591-15643.

474 Zotter, P., El-Haddad, I., Zhang, Y., Hayes, P.L., Zhang, X., Lin, Y.-H., Wacker, L.,
475 Schnelle-Kreis, J., Abbaszade, G., Zimmermann, R., Surratt, J.D., Weber, R., Jimenez,
476 J.L., Szidat, S., Baltensperger, U., Prévôt, A.S.H., 2014b. Diurnal cycle of fossil and
477 nonfossil carbon using radiocarbon analyses during CalNex. *J. Geophys. Res.* 119,
478 6818-6835.

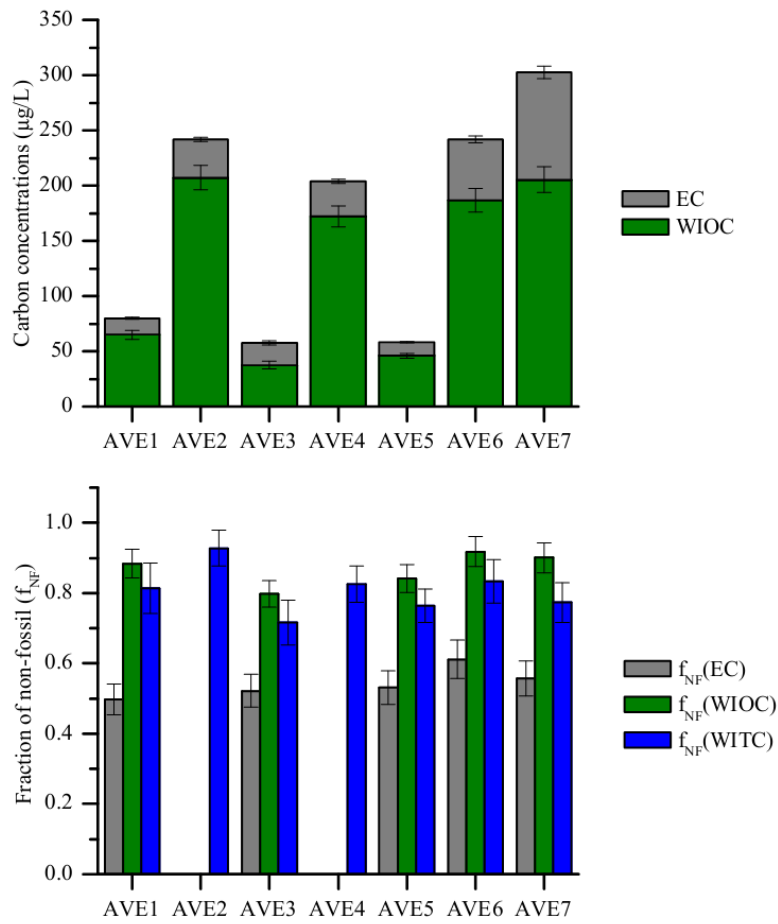


479

480 **Figure 1:** A simplified sketch showing the sources and wet deposition of carbonaceous

481 particles (organic and elemental carbon).

482

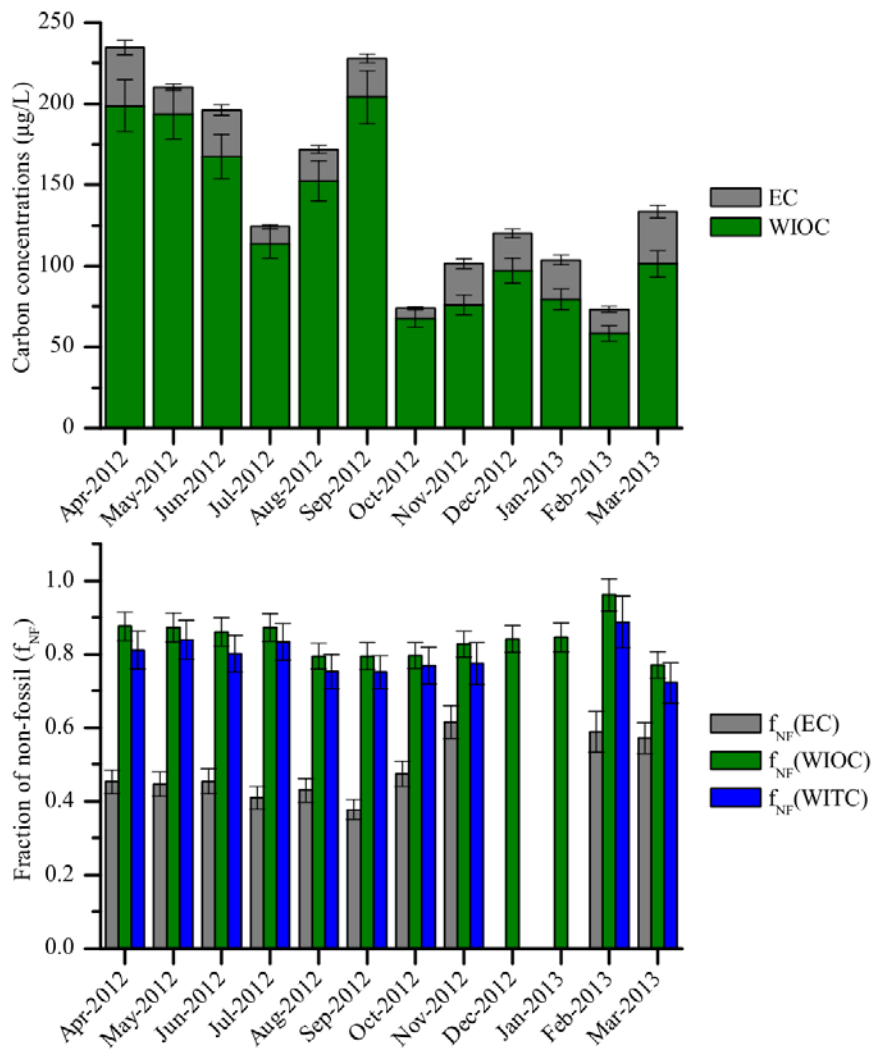


483

484 **Figure 2.** WIOC and EC concentrations and fraction of non-fossil (f_{NF}) values of

485 WIOC, EC and WITC for rain samples collected at Aveiro, Portugal.

486



487

488 **Figure 3.** Monthly WIOC and EC concentrations and fraction of non-fossil (f_{NF}) values
 489 of WIOC, EC and WITC for precipitation samples collected at Dübendorf, Switzerland.